Published in final edited form as:
J Am Chem Soc. 2008 July 23; 130(29): 9240–9241. doi:10.1021/ja8036349.

Ternary I–III–VI Quantum Dots Luminescent in the Red to Near Infrared

Peter M. Allen and **Moungi G. Bawendi***
Department of Chemistry, Massachusetts Institute of Technology, 77 Massachusetts Avenue, Cambridge, Massachusetts 02139

Abstract

We report the synthesis of a size series of copper indium selenide quantum dots (QDs) of various stoichiometries exhibiting photoluminescence (PL) from the red to near infrared (NIR). The synthetic method is modular and we have extended it to the synthesis of luminescent silver indium diselenide QDs. Previous reports on QDs luminescent in the NIR region have been primarily restricted to binary semiconductor systems, such as InAs, PbS, and CdTe. This work seeks to expand the availability of luminescent QD materials to ternary I–III–VI semiconductor systems.

We report the synthesis of a size series of copper indium selenide (Cu–In–Se) quantum dots (QDs) of various stoichiometries exhibiting photoluminescence (PL) from the red to the near infrared (NIR). The synthetic method is modular and we have extended it to the synthesis of luminescent $AgInSe_2$ QDs. Previous reports on QDs luminescent in the NIR region have been primarily restricted to binary semiconductor systems, such as InAs, PbS, and CdTe.[1–3] This work seeks to expand the availability of luminescent QD materials to ternary I–III–VI semiconductor systems. Ternary I–III–VI QDs with tunable band gaps (E_g) in the NIR region are of interest for applications in photovoltaic cells and as biological imaging agents.[4,5]

In bulk Cu–In–Se semiconductors, band edge PL is rarely observed at room temperature due to fast non-radiative relaxation promoted by defect sites.6 Previous work on Cu–In–Se QDs has not reported PL.7–9 Reports on I–III–VI sulfide QD systems have incorporated zinc in order to enhance quantum yields (QYs) and tune emission properties.[10,11] Here, we present a ternary semiconductor system where PL is tuned by QD size.

Previous Cu–In–Se QD synthetic work has included the use of single source precursors.[8] However, the synthetic methodology using single source precursors was not amenable to the facile introduction of capping ligands, preventing adequate size control and surface passivation. Other reports have utilized CuCl, $InCl_3$, and tri-n-octylphosphine selenide (TOPSe) to synthesize Cu–In–Se QDs, but did not produce QDs with distinct absorption features.[7,9] Mechanistic studies on the role of TOPSe in a 'hot injection' QD synthesis has demonstrated two potential reaction pathways for the formation of QDs: (i) the generation of M^0 before reaction with TOPSe and (ii) the direct reaction of carboxylic/phosphonic acid ligands with TOPSe.[12,13] In the absence of these pathways, TOPSe may not be an adequate precursor in combination with CuCl and $InCl_3$ for a 'hot injection' Cu–In–Se QD synthesis.

In our synthetic approach we have selected bis(trimethylsilyl) selenide [$(Me_3Si)_2Se$], as the chalcogenide precursor. The choice of copper precursors was limited by the tendency of Cu(I) to disproportionate in solution.[14] Previous reports have demonstrated that copper and indium

E-mail: mgb@mit.edu.

halides are stable sources of Cu(I) and In(III). 7,9 A combination of metal halides and a chalcogenide silane precursor was selected in order to exploit a metathetical dehalosilylation reaction scheme, eliminating the need to generate elemental copper and indium in solution.15

A combination of tri-n-octylphosphine (TOP) and oleyl amine (OA) was used as a coordinating solvent. The metal halides can be readily dispersed in TOP or OA to form homogeneous solutions. In a typical synthesis, a solution of metal halides in TOP and OA was heated to 280–360 °C followed by the swift injection of a solution of $(Me_3Si)_2Se$ in TOP and subsequent growth at temperatures ranging from 200–280 °C. The size and composition of the prepared QDs can be tuned by the choice of metal halides and growth temperatures.

The CuI and InI_3 precursors produced QDs of composition $CuIn_5Se_8$, with PL in the red and NIR (Figure 1a). The elemental compositions of the QDs resulting from the reaction of the iodide precursors with $(Me_3Si)_2Se$ were found to be largely independent of reaction conditions (Figure S1). In the case of the CuCl and $InCl_3$ precursors it was possible to tune the composition of the prepared QDs from $CuIn_{1.5}Se_3$ to $CuIn_{2.3}Se_4$ (Figure 1b) by varying the reaction temperature (Table S1). This synthetic method produced a size series of Cu–In–Se QDs of various stoichiometries luminescent from the red to NIR (Figure 2a). The generality of this synthetic approach was demonstrated by replacing the metal halide precursors with AgI and InI_3, which successfully synthesized $AgInSe_2$ QDs with luminescence from orange to red (Figure S2).

Transmission electron microscopy (TEM) indicates the QDs are spherical in nature with an approximately 15% rms deviation in size from the mean QD diameter (Figure 2b, Figure S3). The sizes determined by TEM measurements are in agreement with those obtained by Scherrer analysis, suggesting the crystalline coherence length extends over the entire QD.

Bulk Cu–In–Se exists primarily in either a tetragonal chalcopyrite or a high temperature cubic sphalerite phase.[16] The observed wide angle X-ray scattering (WAXS) and elemental compositions of the Cu–In–Se QDs were found to be well described by an ordered vacancy chalcopyrite (OVC) structure. Analysis of 6 nm $CuIn_{1.5}Se_3$ QDs WAXS data began by creating a chalcopyrite model unit cell using experimentally determined copper, indium, and selenium stoichiometries. Copper vacancies (V_{Cu}) were initially placed exclusively on the copper site, resulting in the calculated pattern in Figure 3a. However, the calculated intensities for the (211) and (101) reflections in this model structure exceed the observed WAXS intensities. The indium atoms were then allowed to migrate onto the copper site (In_{Cu}) until the calculated pattern was in agreement with the observed pattern (Figure 3b). A structural model containing In_{Cu} and $2V_{Cu}$ defect pairs is in agreement with an ordered vacancy chalcopyrite (OVC) phase. The elemental compositions of all the Cu–In–Se QDs are consistent with the predicted stoichiometries for ordered vacancy CU-IN-SE compounds (Table S2).[17] An alternative cubic sphalerite model unit cell does not adequately describe the observed WAXS pattern (Figure 3c). Attempt at a similar WAXS analysis for smaller Cu–In–Se QDs was complicated by increased broadening of the (211) and neighboring reflections (Figure S4).

The assignment of $CuIn_{1.5}Se_3$ and $CuIn_{2.3}Se_4$ QDs as chalcopyrite compounds is in agreement with the previously reported chalcopyrite phases of bulk $CuInSe_2$ and $CuIn_3Se_5$.[18] As for $CuIn_5Se_8$, only a metastable chalcopyrite phase has been reported in the bulk. Over the crystalline coherence lengths in this work (2–6 nm) chalcopyrite Cu–In–Se QDs were observed over a large range of stoichiometries. In the case of the $AgInSe_2$ QDs WAXS patterns it was not possible to distinguish between orthorhombic and hexagonal phases due to the small (3–6 nm) crystalline coherence lengths (Figure S5). $AgInSe_2$ nanorods have previously been reported in an orthorhombic phase.[19]

The observation of PL from Cu–In–Se QDs (QYs up to 25% and decreasing significantly with increasing size) may arise due to the strong confinement of the exciton within the QD. Radiative pathways in the Cu–In–Se QDs appear to remain competitive even in the presence of structural defects, which are known to promote non-radiative relaxation in bulk Cu–In–Se.[6] In addition, QYs of the $AgInSe_2$ QDs reached 15%.

The broad PL (~100 nm fwhm) observed in the Cu–In–Se QDs arises at least in part from a distribution of QD sizes. It is also possible that a distribution of near band edge trap states, known to arise from shallow donor acceptor pairs created by defects and vacancies, contributes to the broad PL.[17]

In the bulk, $CuInSe_2$, $CuIn_3Se_5$, and $CuIn_5Se_8$ have been reported with E_g values of 1.04 eV, 1.21 eV, and 1.15 eV, respectively.[18] The E_g of Cu–In–Se QDs has been tuned here from 1.3–1.94 eV (975–640 nm), which is to the blue of the bulk E_g values (Figure S6). We conclude that quantum confinement plays a significant role in determining the E_g of Cu–In–Se QDs,[20] while differing elemental compositions may contribute additional small E_g energy variations similar to bulk Cu–In–Se.

The range of E_g values demonstrated by the Cu–In–Se in this work is comparable to the range attainable by thin film copper indium gallium selenide semiconductors (1.0–1.7 eV), which are used in photovoltaic devices.[21] In addition, the small size and NIR emission of Cu–In–Se QDs make them potentially desirable for biological imaging applications.5 The growth of a passivating shell around the Cu–In–Se QDs could enable surface ligand modifications.

In conclusion, we have developed a modular hot injection synthetic method for ternary QDs, composed of commercially available precursors. This synthetic method has the potential to be extended to other QDs composed of I–III–VI semiconductors, allowing for further exploration of the elemental compositions and electronic properties in QD materials.

Supplementary Material

Refer to Web version on PubMed Central for supplementary material.

Acknowledgments

We thank S. Speakman for assistance with WAXS. This work was supported in part by the MIT-Harvard NIH CCNE (1U54-CA119349), the US ARO through the ISN (DAAD-19-02-0002) and the NSF NSEC (DMR-0117795). This work also made use of the shared experimental facilities of the NSF MRSEC program (DMR-0213282) at MIT.

References

1. Murray CB, Norris DJ, Bawendi MG. J. Am. Chem. Soc 1993;115:8706–8715.
2. Guzelian AA, Banin U, Kadavanich AV, Peng X, Alivisatos AP. Appl. Phys. Lett 1996;69:1432–1434.
3. Hinds S, Myrskog S, Levina L, Koleilat G, Yang J, Kelley SO, Sargent EH. J. Am. Chem. Soc 2007;129:7218–7219. [PubMed: 17503821]
4. Huynh WU, Dittmer JJ, Alivisatos AP. Science 2002;295:2425. [PubMed: 11923531]
5. Zimmer JP, Kim SW, Ohnishi S, Tanaka E, Frangioni JV, Bawendi MG. J. Am. Chem. Soc 2006;128:2526–2527. [PubMed: 16492023]
6. Shigefusa C. Appl. Phys. Lett 1997;70:1840–1842.
7. Malik MA, O'Brien P, Revaprasadu N. Adv. Mater 1999;11:1441.
8. Castro SL, Bailey SG, Raffaelle RP, Banger KK, Hepp AF. Chem. Mater 2003;15:3142–3147.
9. Zhong H, Li Y, Ye M, Zhu Z, Zhou Y, Yang C, Li Y. Nanotechnology 2007;18:025602.
10. Nakamura H, Kato W, Uehara M, Nose K, Omata T, Otsuka-Yao-Matsuo S, Miyazaki M, Maeda H. Chem. Mater 2006;18:3330.

11. Torimoto T, Adachi T, Okazaki Ki, Sakuraoka M, Shibayama T, Ohtani B, Kudo A, Kuwabata S. J. Am. Chem. Soc 2007;129:12388–12389. [PubMed: 17887678]
12. Steckel JS, Yen BKH, Oertel DC, Bawendi MG. J. Am. Chem. Soc 2006;128:13032–13033. [PubMed: 17017765]
13. Liu H, Owen JS, Alivisatos AP. J. Am. Chem. Soc 2007;129:305. [PubMed: 17212409]
14. Courtney WG. J. Phys. Chem 1956;60:1461–1462.
15. Wells RL, Pitt CG, McPhail AT, Purdy AP, Shafieezad S, Hallock RB. Chem. Mater 1989;1:4–6.
16. Schumann B, Tempel A, Kühn G. Cryst. Res. Technol 1988;23:3.
17. Zhang SB, Wei S–H, Zunger A, Katayama-Yoshida H. Phys. Rev. B 1998;57:9642–9656.
18. Wasim SM, Rincon C, Marin G, Delgado JM. Appl. Phys. Lett 2000;77:94–96.
19. Ng MT, Boothroyd CB, Vittal JJ. J. Am. Chem. Soc 2006;128:7118–7119. [PubMed: 16734438]
20. Brus LE. J. Chem. Phys 1984;80:4403–4409. (b) The effective mass approximation overstates the degree of quantum confinement for the small QDs (radii 1.0–1.5 nm) presented in this work.
21. Ramanathan K, Teeter G, Keane JC, Noufi R. Thin Sol. Films 2005;480–481:499–502.

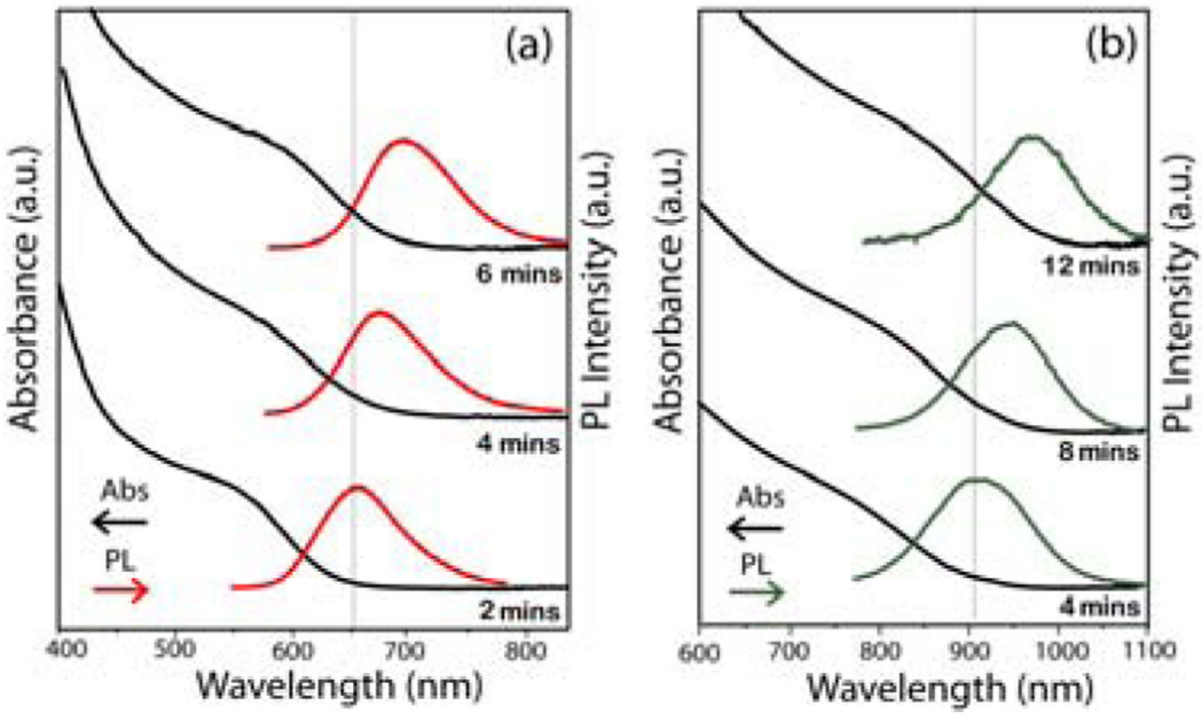

Figure 1.

Absorbance and PL of: (a) $CuIn_5Se_8$ QDs grown from 650–700nm with injection at 280 °C and growth at 210 °C from CuI and InI_3 precursors and (b) $CuIn_{2.3}Se_4$ QDs grown from 900–975 nm with identical conditions as in (a) but with CuCl and $InCl_3$ precursors.

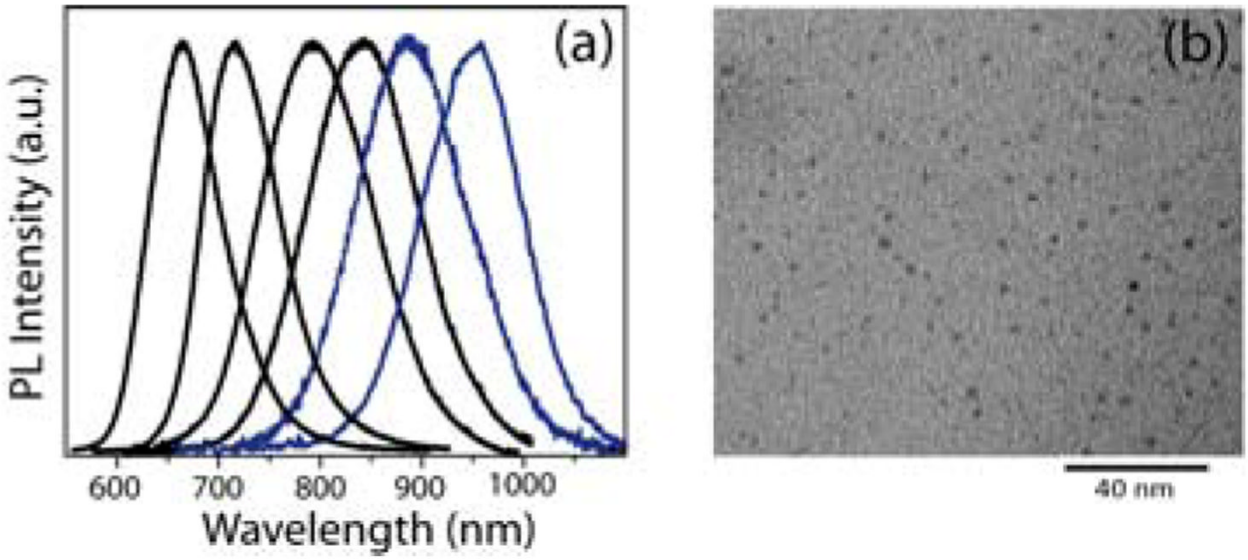

Figure 2.
(a) PL spanning from the red to the NIR (650–975 nm) from $CuIn_5Se_8$ QDs ranging from ~2.0–3.5 nm mean diameter (black) and from $CuIn_{2.3}Se_4$ QDs (~3.0–3.5 nm mean diameter) (blue). (b) TEM of 3.0 +/− 0.5 nm $CuIn_{2.3}Se_4$ QDs.

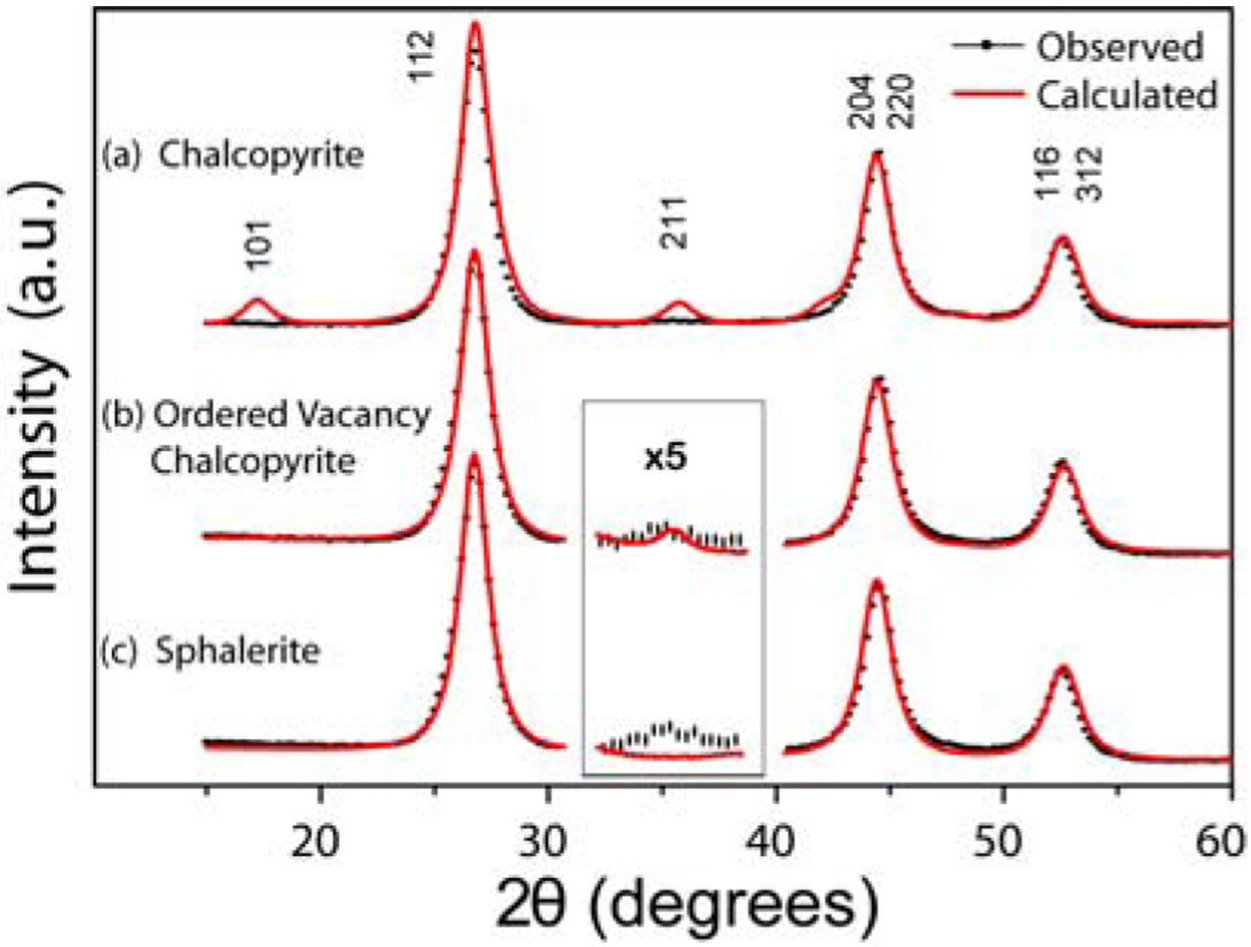

Figure 3.

Comparison of experimental WAXS to calculated patterns for model unit cells of $CuIn_{1.5}Se_3$ QDs (6 nm diameter by Scherrer analysis). (a) The calculated pattern for a chalcopyrite phase where the calculated intensity of the (211) and (101) reflections exceed the observed intensity, (b) is the calculated pattern for an ordered vacancy chalcopyrite phase in agreement with the observed WAXS pattern, and (c) is a calculated cubic sphalerite phase that lacks the (211) reflection.